



s -Process signatures in bulk presolar silicon carbide: a multielement study

U. Ott¹, Q.-Z. Yin², and C.-T. Lee³

¹ Max-Planck-Institut für Chemie (Otto-Hahn-Institut), Becherweg 27, D-55128 Mainz, Germany; e-mail: ott@mpch-mainz.mpg.de

² Department of Geology, University of California at Davis, Davis, CA 95616, USA

³ Department of Earth Sciences, Rice University, Houston, TX 77005, USA

Abstract. Isotopic and elemental abundance signatures in the mass range Sr through Hf have been determined in a silicon carbide-rich sample of the Murchison carbonaceous chondrite, using inductively-coupled plasma mass spectrometry (ICP-MS). Despite the problem of isobaric interferences useful results were obtained for a number of isotopes, several for the first time. While disagreements between astrophysical predictions and earlier results for ¹³⁷Ba and ¹⁴⁶Nd obtained by thermal ionization mass spectrometry are confirmed, our data for Dy are in line with predictions. A hint is observed for *in-situ* decay of ¹⁰⁷Pd produced in the s -Process. The elemental abundance pattern shows deficits relative to production ratios of volatile elements including the more volatile Rare Earth Elements (REE). Very refractory elements including the abundant (in absolute terms) element Zr appear to be underabundant relative to refractory REE such as Nd.

Key words. nucleosynthesis: s -Process, abundances - meteors - stars: AGB, carbon - presolar grains: silicon carbide

1. Introduction

The first isotopic analyses of elements in SiC showing the signature of the s -Process (other than Kr and Xe) were made on aggregates of (many) SiC grains by thermal ionization mass spectrometry (TIMS) and by SIMS (Ott & Begemann 1990a, b, Zinner et al. 1991, Prombo et al. 1993). For a summary of these results that were obtained for the elements Sr, Ba, Nd, Sm and Dy see Hoppe & Ott (1997). The study of single grains for the more abundant elements was made possible with the development of resonance ionization mass spec-

trometry (RIMS) by Nicolussi et al. (1997) and applied to the study of Sr, Zr, Mo, Ru and Ba (Nicolussi et al. 1997, 1998a, 1998b, Savina et al. 2003, 2004). Because of its relatively high abundance and good ionization yield it has also been possible to analyze Ba in single SiC grains by the NanoSIMS (Marhas et al. 2003, 2005).

Almost all of these isotopic analyses of s -Process elements, however, whether on single grains or aggregates were more or less one-element studies. Here we report on the application of inductively coupled plasma mass spectrometry (ICP-MS), a multielement technique, by which we have obtained data in the mass range from Sr to Hf. A drawback of the

Send offprint requests to: U.Ott

method is the fact that in analyses of multielement samples there is abundant isobaric interference. Nevertheless, our results for the subset of isotopic pairs that are free from interferences or where corrections can be applied with confidence provide valuable information. Since the technique was performed on many grains, the results should provide a representative average pattern of the *s*-Process in presolar SiC, not only concerning isotopic compositions, but also the elemental abundance pattern.

Results for the Ba through Hf region are reported in more detail in Yin et al. (2006), where also details regarding the sample and the experimental procedures are given.

2. Isotopes: Barium through hafnium

We succeeded in clearly observing the signature of the *s*-Process in a number of elements: Ba, Nd, Dy, and for the first time Er and Hf. Except for Hf, which is dominated by normal Hf and where *s*-Process Hf makes only a small (few %) contribution, the ratio of pure *s*-Process to isotopically normal component is typically $\sim 2:1$. No clear indications were seen in the other elements because of one or more of the following reasons: a) elements are mono-isotopic or nearly so (La, Ce, Pr, Tb, Ho, Tm); b) low abundance (Sm, Eu, Yb); c) problems with molecular or isobaric interferences (Sm, Eu, Gd).

The new results allow to check for consistency with previous analytical results for “bulk SiC” obtained by thermal ionization mass spectrometry (TIMS) or secondary ion mass spectrometry (SIMS) and for comparison with results from model calculations based on either the classical approach or the stellar model. The most relevant source for comparison with theoretical considerations is Arlandini et al. (1999), where it has to be kept in mind that these authors tried to reproduce the solar system abundance distribution, which is characterized by a higher neutron exposure than the *s*-Process observed in SiC (~ 0.30 vs. 0.15 mb^{-1} ; cf. Gallino et al. 1993). As for isotopic compositions, this affects essentially only Ba, because the abundance of ^{138}Ba with its small capture cross section is sensitive to neutron ex-

posure. The difference is, however, also important in interpreting the elemental abundance pattern (see below).

2.1. Barium and neodymium

Of interest are the ratios $^{137}\text{Ba}/^{136}\text{Ba}$ and $^{146}\text{Nd}/^{144}\text{Nd}$ because of previous discrepancies between theoretical expectations and analytical results obtained by TIMS. Our new results confirm the TIMS results for the Ba ratio precisely, and also for the Nd ratio they are close to the TIMS data. As for the other isotopic ratios, where data are available, both new and old analytical data are consistent with theory. This is true, in particular, also for the low $^{138}\text{Ba}/^{136}\text{Ba}$, which is the mark of the low neutron exposure characteristic for the *s*-Process in presolar SiC.

2.2. Dysprosium

Dysprosium is an interesting element because of the bound-state β -decay of ^{163}Dy , which leads to a branching that affects the abundances of ^{163}Dy , ^{164}Dy and ^{164}Er . Previous measurements of bulk SiC by TIMS indicated much lower $^{163}\text{Dy}/^{162}\text{Dy}$ and $^{164}\text{Dy}/^{162}\text{Dy}$ ratios than expected from calculations. Our new data are shown in Fig. 1 and suggest perfect agreement with theory in ^{163}Dy , while the situation for ^{164}Dy appears somewhat ambiguous.

2.3. Erbium and hafnium

No useful data were obtained for the interesting isotope ^{164}Er because it cannot be resolved from ^{164}Dy (expected to be much more abundant) in our experiment. The relative abundances of ^{166}Er , ^{167}Er , ^{168}Er and ^{170}Er (after minor corrections for ^{168}Yb and ^{170}Yb) are in perfect agreement with expectations. As for Hf, while the contribution of the *s*-Process is clearly visible, it is too small to derive a meaningful isotopic composition for *s*-Process Hf.

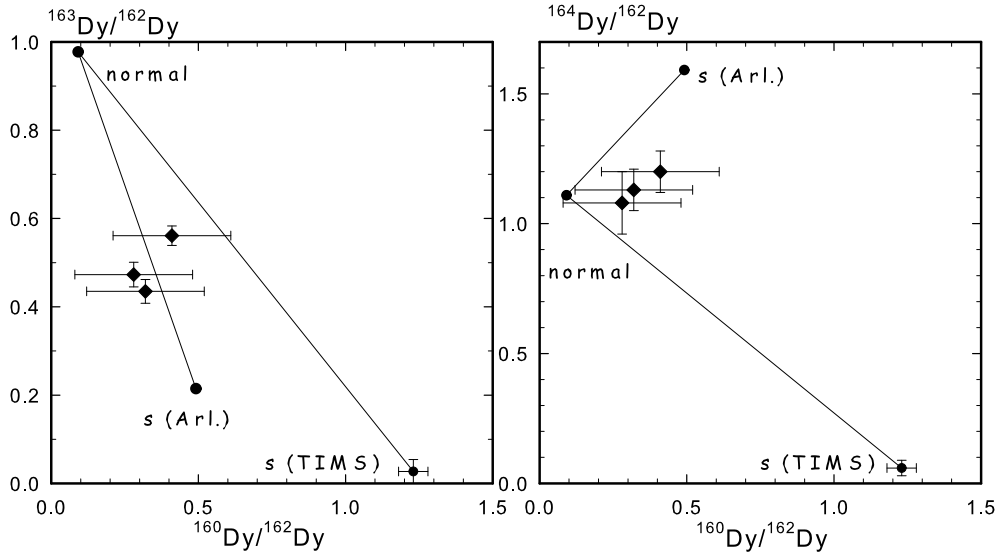


Fig. 1. Plots of $^{163}\text{Dy}/^{162}\text{Dy}$ (left) and $^{164}\text{Dy}/^{162}\text{Dy}$ (right) vs. $^{160}\text{Dy}/^{162}\text{Dy}$. Murchison SiC data: full diamonds. Also shown are mixing lines between normal composition (de Laeter et al. 2003) and both, the *s*-Process composition according to the stellar model of Arlandini et al. (1999), and that derived from previous TIMS work.

3. Elemental abundance ratios: Ba through Hf

The data obtained in the Ba through Hf region allow construction of an abundance curve of the *s*-Process component, which can be compared to production ratios. The result is shown in Fig. 2 (right). To eliminate the dilution effect in Hf, for all elements the abundance of the pure *s*-Process component has been used as derived from the isotopic patterns. In addition upper limits are given for some elements. Normalization is to the nuclide ^{144}Nd . The comparison is made not relative to the Arlandini et al. (1999) production ratios because, as noted above, Arlandini et al. aim to reproduce the solar system abundance pattern. This pattern is characterized by an approximately twice as high neutron exposure as the *s*-Process signature in SiC grains, as established

from the results for the Ba isotopes (Ott & Begemann 1990, Gallino et al. 1993, Prombo et al. 1993). Instead we compare to predictions based on a semi-classical model with neutron exposure 0.15 mb^{-1} . Because of the large neutron capture cross sections in the REE region, predictions are virtually identical there (on the scale of interest) with those of Arlandini et al. (1999), and the only noticeable difference is in Ba/Nd.

Remarkably, quite a few of the well-determined abundance ratios fall close to the $\equiv 1$ line, indicating capture by the SiC grains (on average) of REE in the ratios as produced. Also monoisotopic Pr and almost monoisotopic La and Ce, which together with Ba and Nd are located on the second *s*-Process abundance peak, are extremely close to the line, if a mixture 2:1 between pure *s*-Process component and normal is assumed, as observed for

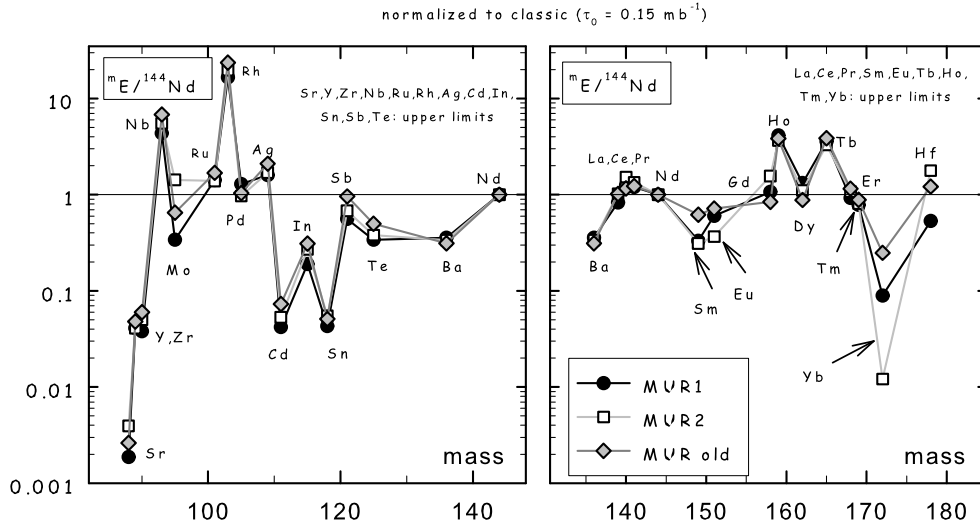


Fig. 2. Elemental abundance pattern of *s*-Process component in SiC, normalized to ^{144}Nd and expectations from a classical model with neutron exposure $\tau_0 = 0.15 \text{ mb}^{-1}$. Left: mass range from Sr to Nd; right: Ba to Hf. Nuclides plotted are ^{88}Sr , ^{89}Y , ^{90}Zr , ^{93}Nb , ^{95}Mo , ^{101}Ru , ^{103}Rh , ^{105}Pd , ^{109}Ag , ^{111}Cd , ^{115}In , ^{118}Sn , ^{121}Sb , ^{125}Te , ^{136}Ba , ^{139}La , ^{140}Ce , ^{141}Pr , ^{144}Nd , ^{149}Sm , ^{151}Eu , ^{158}Gd , ^{159}Tb , ^{162}Dy , ^{165}Ho , ^{168}Er , ^{169}Tm , ^{172}Yb , ^{178}Hf .

Ba, Nd, Dy and Er (see above). Exceptions are elements that are more volatile: Ba, and the REE Sm, Eu, and in particular Yb, the most volatile of the REE.

Ba and the REE are expected to condense in carbon star atmospheres as sulfides into preexisting SiC, where they form solid solutions, with condensation temperatures under conditions of solid solution formation with SiC increased as compared to the case of simple sulfide condensation (Lodders & Fegley 1995). Dedicated calculations such as those of Lodders & Fegley (1995, 1997) but covering the full REE range could be used in principle to define an exact condensation temperature from this pattern (for a given pressure).

4. Sr to Te with a hint for extinct ^{107}Pd

The mass range below Ba has proven to be a lot more difficult for our type of approach and safe results are only upper limits for the *s*-Process contribution to elements in this mass range. There are several reasons for this. For one, many of the elements (Te, Sb, Sn, Cd, Ag, Sr) below Ba are even more volatile than Ba and the most volatile of the REE, which, when compared to production ratios, already have been found to be depleted in SiC relative to the more refractory ones (see above). They may simply be absent from SiC. Others (Zr, Mo, Ru, Pd) are chemically resistant, either as elements or compounds, and a significant fraction of normal solar system matter for these elements has survived the chemical extraction procedure together with SiC, thus diluting any *s*-Process signature from the SiC grains (Y, Nb

Table 1. Ag isotopic composition measured in SiC rich sample by ICP-MS.

Sample	Mur 1	Mur 2	Mur old	normal
$^{107}\text{Ag}/^{109}\text{Ag}$	1.20 ± 0.03	1.15 ± 0.03	1.14 ± 0.02	1.076

and Rh, in addition, are monoisotopic.) Among these, molybdenum, in effect, has been shown to be present by the RIMS analyses of individual SiC grains (Nicolussi et al. 1998a), and a small hint may be seen in our data, as for Pd.

The interesting case in this mass range may be silver. Results are listed in Table 1.

Because of the small signals, and because of variable interferences observed in the general mass region (most severely affecting Cd), the results have to be treated with some caution and need to be confirmed. Taken at face value they suggest an overabundance of roughly 10% (relative to normal) of ^{107}Ag . This cannot be due to addition of *s*-Process Ag, for which Arlandini et al. (1999) predict a ratio of ~ 0.64 . It may, however, indicate the presence of live ^{107}Pd at the time of grain formation, which would have been introduced with the other stable isotopes of Pd, an element more refractory than Ag. Assuming, because of its volatility, no *s*-Process Ag to be present and the background to consist of isotopically normal Ag, a rough estimate for the $^{107}\text{Pd}/^{108}\text{Pd}$ ratio of the *s*-Process component at the time of grain formation can be made based on these data and the small indication for *s*-Process Pd. The results for our three samples (~ 0.07 - 0.10) compare quite favorably with the production ratio in the *s*-Process, which is predicted to be in the range 0.11-0.14 (Wasserburg et al. 2006).

The elemental abundance pattern for the Sr to Nd range, mostly upper limits, normalized to that expected from a classical *s*-Process with neutron exposure $\tau_0 = 0.15 \text{ mb}^{-1}$ and normalized to ^{144}Nd , is shown on the left hand side of Fig. 2, analogous to that for the Ba through Hf range on the right in Fig. 2. Notably not only the volatile elements are underabundant (where the upper limit is low enough for such a conclusion), but also refractory Y and Zr, although

the latter is quite abundant in absolute terms so that it could be measured in single grains using RIMS (Nicolussi et al. 1997).

5. Summary

Applying ICP-MS, a multielement mass spectrometric technique, we have investigated a SiC-rich sample of the Murchison meteorite for *s*-Process contributions in the mass range from Sr to Hf. In the heavier mass region, Ba and above, clear *s*-Process signatures have been observed for a number of elements. The data allow the construction of an abundance curve (upper limits only for various elements) that shows the effect of volatility in that the more volatile elements (including the more volatile REE) appear to be low in abundance relative to the reference element, neodymium, and to production ratios from the *s*-Process. Interestingly, also highly refractory Zr appears to be underabundant. Isotopic data inferred for the *s*-Process component generally agree with expectations, although previously observed discrepancies between analyses and expectations for $^{137}\text{Ba}/^{136}\text{Ba}$ and $^{146}\text{Nd}/^{144}\text{Nd}$ persist. Isotopic data for Dy seem in line with expectations and suggest analytical problems in the earlier TIMS work. The data also provide a hint for the presence of live ^{107}Pd at the time of SiC grain formation.

References

- Arlandini, C., Käppeler, F., Wisshak, K., Gallino, R., Lugaro, M., Busso, M., Straniero, O. 1999, *ApJ*, 525, 886
- De Laeter, J.R., Böhlke, J.K., De Bièvre, P., Hidaka, H., Peiser, H.S., Rosman, K.J.R.,

- Taylor, P.D.P. 2003, *Pure Appl. Chem.*, 75, 683
- Gallino, R., Raiteri, C.M., Busso, M. 1993, *ApJ*, 410, 400
- Hoppe, P., Ott, U. 1997, in *Astrophysical Implications of the Laboratory Study of Presolar Materials*, eds. T.J. Bernatowicz, E. Zinner (Woodbury, NY: American Institute of Physics), p. 27
- Lodders, K., Fegley, B., Jr. 1995, *Meteoritics*, 30, 661
- Lodders, K., Fegley, B., Jr. 1997, in *Astrophysical Implications of the Laboratory Study of Presolar Materials*, eds. T.J. Bernatowicz, E. Zinner (Woodbury, NY: American Institute of Physics), p. 391
- Marhas, K.K., Hoppe, P., Ott, U. 2003, *Meteorit. Planet. Sci.*, 38, A58
- Marhas, K.K., Hoppe P., Ott, U. 2005, *Lunar Planet. Sci.*, 36, CD-ROM Abstract 1855
- Nicolussi, G.K., Davis, A.M., Pellin, M.J., Lewis, R.S., Clayton, R.N., Amari, S. 1997, *Science*, 277, 1281
- Nicolussi, G.K., Pellin, M.J., Lewis, R.S., Davis, A.M., Amari, S., Clayton, R.N. 1998a, *Geochim. Cosmochim. Acta*, 62, 1093
- Nicolussi, G.K., Pellin, M.J., Lewis, R.S., Davis, A.M., Clayton, R.N., Amari, S. 1998b, *Phys. Rev. Lett.*, 81, 3583
- Ott, U., Begemann, F. 1990a, *ApJ*, 353, L57
- Ott, U., Begemann, F. 1990b, *Lunar Planet. Sci.*, 21, 920
- Prombo, C.A., Podosek, F.A., Amari, S., Lewis, R.S. 1993, *ApJ*, 410, 393
- Savina, M.R., Davis, A.M., Tripa, C.E., Pellin, M.J., Clayton, R.N., Lewis, R.S., Amari, S., Gallino, R., Lugaro, M. 2003, *Geochim. Cosmochim. Acta*, 67, 3201
- Savina, M.R., Davis, A.M., Tripa, C.E., Pellin, M.J., Gallino, R., Lewis, R.S., Amari, S. 2004, *Science*, 303, 649
- Wasserburg, G.J., Busso, M., Gallino, R., Nollett, K.M. 2006, *Nucl. Phys. A*, in press.
- Yin, Q.-Z., Lee, C.-T. A., Ott, U. 2006, *ApJ*, submitted
- Zinner, E., Amari, S., Lewis, R.S. 1991, *ApJ*, 382, L47